Ablation of long noncoding RNA MALAT1 activates antioxidant pathway and alleviates sepsis in mice

Jingshu Chen [a],[1], Shu Tang [a],[1], Sui Ke [a], James J. Cai [b], Daniel Osorio [b], Andrei Golovko [c], Benjamin Morpurgo [c], Shaodong Guo [d], Yuxiang Sun [d], Melanie Winkle [e], George A. Calin [e], Yanan Tian [a],[*]

[a] Department of Veterinary Physiology and Pharmacology, Texas A&M University, College Station, Tx, 77843, USA
[b] Department of Veterinary Integrative Biosciences, Texas A&M University, College Station, Tx, 77843, USA
[c] Texas A&M Institute for Genomic Medicine (TIGM), College Station, TX, 77843, USA
[d] Department of Nutrition, Texas A&M University, College Station, Tx, 77843, USA
[e] Department of Translational Molecular Pathology, University of Texas MD Anderson Cancer Center, Houston, Tx, 77230, USA

A B S T R A C T

The metastasis-associated lung adenocarcinoma transcript1 (MALAT1) is a long noncoding RNA (lncRNA) and is known for its role in cancer development and prognosis. In this study, we report that MALAT1 plays an important role in regulating acute inflammatory responses in sepsis. In patient samples, MALAT1 expression was positively correlated with severity of sepsis. In cultured macrophages, LPS treatment significantly induced MALAT1 expression, while genetic ablation of MALAT1 greatly reduced proinflammatory cytokine levels. Furthermore, MALAT1-ablated mice had significantly increased survival rates in cecal ligation and puncture (CLP)-induced sepsis and LPS-induced endotoxemia. One novel and salient feature of MALAT1-ablated mice is greatly reduced ROS level in macrophages and other cell types and increased glutathione/oxidized glutathione (GSH/GSSG) ratio in macrophages, suggesting an increased antioxidant capacity. We showed a mechanism for MALAT1 ablation leading to enhanced antioxidant capacity is through activation of methionine cycle by epitranscriptomical regulation of methionine adenosyltransferase 2A (MAT2A). MAT2A 3′UTR can be methylated by METTL16 which was known to directly bind to MALAT1. MALAT1 ablation was found to reduce methylation in MAT2A hairpin1 and increase MAT2A protein levels. Our results suggest a MALAT1-METTL16-MAT2A interactive axis which may be targeted for treatments of sepsis.

1. Introduction

Sepsis is a disease with high lethality and morbidity [1,2] and the pathogenesis of sepsis is accompanied by profound metabolic disturbances of the redox system, leading to oxidative stress. Oxidative stress as a result of the acute inflammatory responses inherent with sepsis may result in microcirculatory dysfunction, acute respiratory failure, tissue damage, multiple organ failure and death [3–5]. Normally, a comprehensive system of interacting antioxidant defenses is able to counteract with oxidative stress and prevent tissue/organ damage [6]. However, the antioxidant mechanisms may be overwhelmed by the oxidative stress associated with acute immune/inflammatory responses in the sepsis.

One of the major determinants of antioxidant capacity is GSH, which is biosynthesized through methionine cycle [7]. In the GSH synthesis pathway, methionine is sequentially converted to cysteine via several

enzymatic steps, among which, the first and the critical step is conversion of methionine to S-adenosyl methionine (SAM) in a reaction catalyzed by methionine adenosyltransferase (MAT) [8–10]. SAM, as a major precursor of GSH, has been found to restore GSH levels and alleviate LPS-induced inflammatory response in mice [11]. It was recently found that the mRNA of MAT2A, one of the most important MAT enzymes, was post-transcriptionally regulated by RNA methylation writer METTL16 which binds to and methylates 3′ UTR of MAT2A mRNA thus regulating its mRNA level through controlling its intron splicing [12]. Generally, N6-methyladenosine (m^{6}A) methylation of MAT2A is associated with decreased expression by mRNA degradation [12,13]. Interestingly, METTL16 is also found to directly bind to lncRNA MALAT1 on the triple helix structure on its 3' region [14,15]. Thus, it is important to understand how MAT2A is regulated under sepsis, and if MALAT1 regulates MAT2A gene expression through METTL16.

In recent years, development of massively parallel sequencing

technologies provides new possibilities to unravel the regulatory roles of lncRNAs, which are defined as transcripts >200 bp that do not code for proteins [16,17]. MALAT1 is an evolutionarily conserved lncRNA with high level of expression in various tissues and cell types. It has been found to be over-expressed in various cancers and has been considered as a prognostic marker for cancers [18,19]. Accumulating studies demonstrate a subset of lncRNAs are functionally relevant and their dysregulation have significant implications in many inflammatory diseases [20–25]. MALAT1 over expression has also been found to be associated with inflammatory responses [18,26–29]. In an earlier study, we have found that genetic ablation of MALAT1 enhanced the antioxidant capacity, greatly reduced LPS and TNF-α induced oxidative stress, and suppressed oxidative stress-induced JNK pathway and activated AKT pathway leading to sensitized insulin responses in the MALAT1 ablated mouse [30].

In analyzing human clinical data, we found that MALAT1 expression was positively correlated with the inflammatory responses and severity of sepsis [27,31–35]. In this study, using MALAT1 null mouse, we further analyze the mechanistic role of MALAT1 in regulating acute inflammatory response by using LPS-induced endotoxemia and CLP-induced polymicrobial sepsis models. We showed that MALAT1 is a critical factor in regulating development of sepsis, and that genetic deletion of MALAT1 effectively alleviated inflammatory responses in these mouse models with reduced mortality. Oxidative stress and inflammatory responses mutually promote each other. MALAT1 ablation greatly reduced oxidative stress/ROS by enhancing the antioxidant pathways, resulting in suppression of acute inflammatory responses induced by LPS or CLP. We further explored the mechanism of this enhanced antioxidant capacity and found MALAT1 regulated methionine cycle by modulating MAT2A mRNA methylation level. Using the T3 ligation mediated PCR method [36], we found that genetic ablation of MALAT1 significantly reduced the m⁶A methylation and increased MAT2A protein level.

The results of our study indicate that MALAT1 is an important regulator for immune/inflammatory responses, and our results suggest a model of MALAT1 in regulating methionine cycle at epitranscriptomic level through interacting with METTL16 and this interaction is important for post-transcriptionally regulation of MAT2A. This MALAT1-METTL16-MAT2A interactive axis may be targeted for treatment of sepsis through antisense therapeutics against MALAT1, and/or through provision of supplements to enhance methionine cycle.

2. Materials and methods

Reagents. The primary antibodies used include those against p65, p-p65, IκB, p-IκB, IKK, NLRP3, IL-1β and casapase-1 were purchased from Abcam. GammaBind Plus-Sepharose beads were purchased from Amersham Biosciences. L929, THP-1 was purchased from ATCC. iTaq Universal SYBR Green One-step Kit was purchased from Bio-Rad. M⁶A antibody was purchased from Epigentek. FBS, penicillin and streptomycin were purchased from Gibco. T3 ligase was purchased from New England Biolabs. MALAT1 antisense GapmeR was purchased from Qiagen. Mouse cytokine array C3 was purchased from RayBiotech. TNF-α was purchased from Roche. Accutase, Brewer's thioglycollate medium, fluorescent dye 2′,7′-dichlorofluorescein (H2-DCFH-DA), HBSS, histopaque-1077, IMDM, LPS, lysis buffer for Western blot, MILLIPLEX mouse cytokine/chemokine magnetic bead panel - immunology multiplex assay, phorbol 12-myristate 13-acetate (PMA), RPMI 1640 medium were purchased from Sigma. Ammonium chloride solution was purchased from Stemcell technologies. TRIzol reagent was purchased from Thermo Fisher Scientific.

Animals. Wild type C57BL/6 and MALAT1 null mice were from Texas A&M Institute for Genomic Medicine (TIGM) and randomly assigned to different treatments.

Isolation of mouse peritoneal macrophages (PM). PM were isolated according to method previously described [37]. Briefly, mice were i.p.

injected with 1 mL brewer's thioglycollate medium. After three days, treated mice were anesthetized by isoflurane and euthanized by cervical dislocation. 5 mL of cold PBS was injected into the peritoneal cavity, and peritoneal fluid was aspirated by needle syringe. Peritoneal fluid was centrifuged for 10 min (400 g, 4 °C). The cell pellet was resuspended in RPMI medium and allowed to sit for 2 h and then the non-adherent cells were washed away with warm PBS.

Preparation of mouse bone marrow derived macrophages (BMDM). BMDM was obtained according to method described [38]. The mice were anesthetized by isoflurane and euthanized by cervical dislocation. The femur and tibia bones were isolated with peeled off hair, skin, and most of muscle tissue removed. The bones were cut open, and bone marrow was flushed out with a 21G needle and syringe into cold PBS with 2% FBS. The bone marrow was passed through a 70 μm cell strainer in order to remove bone fragments and other tissue. Ammonium chloride solution was used to lyse red blood cells. The collected bone marrow cells were cultured in IMDM supplemented with 10% FBS and 15% filtered L929 cell culture supernatant (containing M-CSF). The BMDM were mature and ready for treatment after 7 days. For M1 activation, BMDM was treated with 100 ng/ml LPS overnight.

Isolation of mouse peripheral blood mononuclear cells (PBMC). Peripheral blood was collected by cardiac puncture of anesthetized mice, and 1:1 diluted with HBSS. PBMC were separated through density centrifugation (400 g, 20°C, 30 min) using histopaque-1077 gradient. The interphase fraction containing PBMCs was aspirated, and red blood cells were lysed with ammonium chloride solution. After centrifugation (200 g, 5 min), pelleted PBMC was resuspended in RPMI medium supplemented with 10% FBS.

Preparation of THP-1 derived macrophages. THP-1 derived macrophages were obtained by culturing the cells in RPMI medium supplemented with 0.05 mM 2-mercaptoethanol and 10% FBS containing 100 nM PMA for 24 h. Then the cells were continued to culture in the medium without PMA for additional 3 days. For M1 activation, the macrophages were treated with 100 ng/ml LPS overnight.

ROS measurement by fluorescence microscope, plate reader, and flow cytometry. To determine the ROS level, fluorescent probe H2-DCFH-DA was added to the cell culture (final concentration of 5 μM, 37 °C, 45 min) [39] and fluorescent signals were determined by images analysis with an inverted fluorescence microscope (Olympus IX71), signals were recorded and quantified by a fluorescence microplate reader with excitation at 488 nm and emission at 528 nm. For the flow cytometry assay, treated BMDMs were detached from plate by accutase, and left either unstained or stained with H2-DCFH-DA for 30 min. Flow cytometry analysis was performed with CellStream flow cytometer. 488–528_46-C3 channel was used to record fluorescence intensity.

Immunoprecipitation/Western blotting. Immunoprecipitation and Western blotting were performed based on the procedure described [40]. Cells were homogenized in lysis buffer by Dounce homogenizer. After centrifugation (12,000 g, 4 °C, 15 min), supernatant fractions were collected and incubated with antibodies and GammaBind Plus-Sepharose beads for 2 h at 4 °C on a rotary shaker. Proteins were separated by SDS-PAGE and then transferred to a nitrocellulose membrane. Individual proteins were detected with the specified antibodies followed by horseradish peroxidase-conjugated secondary antibodies and visualized by chemiluminescence.

Measurement of cytokine levels with multiplex microbead immunoassay. The levels of cytokines in the culture supernatant fraction of the LPS-treated PM were determined using multiplex microbead immunoassay. A multiplex biometric immunoassay, containing fluorescent dyed microspheres conjugated with a monoclonal antibody specific for a target protein, was used for cytokine measurement according to the manufacturer's instructions (MILLIPLEX mouse cytokine/chemokine magnetic bead panel - immunology multiplex assay). Proinflammatory cytokines including IL-1α, IL-1β, IL-6, TNF-α, IL-12 (p40), IL-12 (p70) were measured. A range of 1.95–32,000 pg/mL recombinant cytokines were used for establishment of standard curves and maximizing the

sensitivity and the assay dynamic ranges. Cytokine levels was determined using a multiplex array reader from Luminex™ Instrumentation System (Bio-Plex Workstation from Bio-Rad Laboratories). The analyte concentration was calculated using software provided by manufacturer (Bio-Plex Manager Software).

Profiling of mouse inflammatory cytokines by cytokine array. The cytokines and their levels were measured using mouse cytokine array C3 based on the manufacture recommendation.

Mouse LPS-induced endotoxemia. Mice was i.p. injected with 30 mg/kg LPS. Their survival status was checked every 6 h. For the methionine treatment group, the mice were administered with 20 mg/kg methionine via gavage after LPS injection; for the control group, 100 μL water was administered instead of methionine.

Cecal ligation and puncture mouse model. The mice were anesthetized by isoflurane, their abdominal hair was removed, and the aera was disinfected by betadine solution. An incision smaller than 1 cm was made to expose and gently pull out the cecum. The cecum was tightly ligated by 50% of its length with suture, and a puncture was made on the ligated cecum by a 20-gauge needle. The cecum was gently squeezed to make sure a small amount of feces extruded before return into the peritoneal cavity. The skin was closed by sutures, and pain-relieving gel was applied to the wound. For the methionine treatment group, the mice were administered with 20 mg/kg methionine via gavage after CLP; for the cycloleucine (cLEU) group, 400 mg/kg cLEU was i.p. injected 2 days before CLP.

M⁶A methylation RNA immunoprecipitation. The LPS-treated BMDM, PM and THP-1 derived macrophages were used for determination of the m⁶A methylation using anti-m⁶A antibody. As the adenine methylation residues were distributed in different segments of MAT2A mRNA, the antibody-precipitated RNA was determined using quantitative reverse transcription PCR (qRT-PCR) with different primer pairs bracketing different segments (5′ region, coding region, stop codon, and 3′UTR end) of MAT2A RNA as previously reported (Table 1). [14].

T3 ligation assay for detection of m⁶A methylation at single nucleotide level. This assay was performed as previously described to detect the presence of m6A modification on RNA [36]. A pair of probes were designed as illustrated in Fig. 6A, each consisted of a primer region and an antisense region. The probes can only be ligated together by T3 ligase if there are no m6A methylation on the target RNA. And a successful ligation will result in a longer product with primer regions on both ends, therefore can be amplified through PCR. On the contrary, if there is m⁶A methylation on the target site, the two probes cannot be ligated together by T3 ligase, and a single primer on the probe will not be efficiently amplified by PCR. The level of m⁶A methylation on target site can be quantitated by the efficiency of ligation, which will be quantitated by PCR.

Real-time PCR. Total RNA of PM, BMDM, PBMC and THP-1 derived macrophage was isolated using the TRIzol according to the manufacturer's protocol. RNA was eluted using 50 μl of RNase-free water and then stored at −80°C. Real-time PCR was performed using iTaq Universal SYBR Green One-step Kit. The primers used were shown in Table 1.

Statistics. All tests were performed using GraphPad Prism software 9. The difference between treatments was determined by *t*-test (between 2 groups) and 2-way ANOVA (between more than 2 groups). The difference between survival rates was determined by Gehan-Breslow-

Table 1
Mouse primers related to inflammation and RNA methylation for qRT-PCR.

Gene Name	Forward Primer	Reverse Primer
Mouse β-ACTIN	GCAACGAGCGGTTCCG	CCCAAGAAGGAAGGCTGGA
Mouse 18S	AACGGCTACCACATCCAAG	CCTCCAATGGATCCTCGTTA
Mouse MALAT1	GGCAGAATGCCTTTGAAGAG	GGTCAGCTGCCAATGCTAGT
Mouse IL-1β	GAAATGCCACCTTTTGACAGTG	TGGATGCTCTCATCAGGACAG
Mouse IL-6	CTGCAAGAGACTTCCATCCAG	AGTGGTATAGACAGGTCTGTTGG
Mouse TNF-α	CTGAACTTCGGGGTGATCGG	GGCTTGTCACTCGAATTTTGAGA
Mouse NLRP3	TGGATGGGTTTGCTGGGAT	CTGCGTGTAGCGACTGTTGAG
Mouse Casspase1	TTGAAAGACAAGCCCAAGGTG	CTGGTGTTGAAGAGCAGAAAGC
Mouse MAT2A	GCTTCCACGAGGCGTTCAT	CATCAGGGTCTTGTTGAAGGTG
Mouse MAT2A 5′ region	GAAGCGATCCTCCCTCTGTG	TCAATGAACGCCTCGTGGAA
Mouse MAT2A coding	TCCACGAGGCGTTCATTGAG	TGCATCAAGGACAGCATCACT
Mouse MAT2A stop codon	CCACTTTGGTAGGGACAGCTT	GGCCCTTTCCCTCAGAGCTT
Mouse MAT2A 3′ end	GGGTTAGACCTACAGGGGGT	TTGCTTAGGGCAAGCAGTCA
Mouse/Human MAT2A hairpin1	TAGCCTTTTTTCCCC	GCTGAAAGAGGACAG
Mouse MAT2A hairpin1 Probe	po4GTAACCTACGCCCTCTATGGGCAGTCGGTGAT	CCATCTCATCCCTGCGTGTCTGAAGGCTTCTrCrU
Human GAPDH	GGTGGTCTCCTCTGACTTCAACA	GTTGCTGTAGCCAAATTCGTTGT
Human MALAT1	GGGGGAGTTTTCAGTATTTTTTTTTG	TACACCTTGAGTCATTTGCCTTTAGG
Human IL-1β	TGATGGCTTATTACAGTGGCAATG	GTAGTGGTGGTCGGAGATTCG
Human MAT2A hairpin1 Probe	po4GTAGCCTACGCCCTCTATGGGCAGTCGGTGAT	CCATCTCATCCCTGCGTGTCTGAAGGCTTCTrCrU
Universal primer for T3 ligation	ATCACCGACTGCCCATAGAG	CCATCTCATCCCTGCGTGTC

Wilcoxon test. All replicates are biology replicates, results were considered significant when p was less than 0.05 at a 95% confidence interval.

Study approval. All animal procedures were approved by IACUC of Texas A&M University, with animal use protocol number IACUC 2020–0050. Animals were maintained according to the NIH guidelines.

3. Results

3.1. Induction of MALAT1 during inflammatory responses in mice and sepsis patients

To understand the role of MALAT1 in the inflammatory process, we determined MALAT1 expression in LPS-treated mouse BMDM and PM by qRT-PCR. The expression of MALAT1 was significantly increased in M1 (pro-inflammatory phase of BMDM) compared to M0 (resting phase of BMDM) (Fig. 1A). Similar induction of MALAT1 by LPS was observed in mouse PBMC (Fig. 1B), consistent with the results from human monocyte THP-1 derived macrophage (Fig. 1C). MALAT1 level was significantly upregulated in response to LPS treatment in a time-dependent manner in mouse PM (Fig. 1D). In analyzing the human whole blood RNA-seq data (GSE138712), we found that MALAT1 expression was significantly increased in the late-onset sepsis patients (Fig. 1E). MALAT1 is also found increased in human bone marrow treated with LPS (Supplemental Fig. 1) [41]. Interestingly, MALAT1 expression was also found to increase in single cell transcriptomic analysis of alveolar macrophages in COVID-19 patients with severe symptom than those with mild symptom (GSE128003), as shown in the t-distributed stochastic neighbor embedding (t-SNE) plot (Fig. 1F). Collectively, these results indicate that MALAT1 levels were closely correlated with pro-inflammatory responses in both mouse and human cells, and in clinical sepsis patients, suggesting MALAT1 plays a critical role in inflammatory responses in sepsis.

3.2. Ablation of MALAT1 inhibits proinflammatory responses

Results from ours (Fig. 1) and others [42] suggest that MALAT1 plays a critical role in regulating immune/inflammatory responses during the progression of sepsis. To further investigate this possibility, we utilized MALAT1−/− PM isolated from genetic MALAT1 knockout mice. The isolated PM from MALAT1 null mice and wild type mice were treated with LPS in vitro. The expression of pro-inflammatory genes including IL-1β, IL-6, and TNF-α were significantly reduced in MALAT1 ablated PM (Fig. 2A–C). This result consisted with the down regulated IL-1β expression in MALAT1 antisense GapmeR knocked down THP-1 derived macrophages (Supplemental Fig. 2A). Next, macrophage-secreted cytokine levels in culture supernatant was collected in the cultured PM after stimulation with LPS (5 μg/mL, 2 h, 4 h, 6 h, 8 h). Consistent with the qRT-PCR results (Fig. 2A–C), we found that the pro-inflammatory cytokines IL-1β, IL-6, TNF-α protein levels were significantly reduced in MALAT1 ablated PM (Fig. 2D–F). To further profile the LPS-induced cytokines, the cytokine antibody arrays were used to examine the levels of 42 cytokines related to immunity and inflammation in culture supernatant of PM. We found MALAT1 ablation broadly inhibited pro-inflammatory cytokines (i.e., CXCL1, MIP-1α, MIP-1γ, MIP-2, IL-6) secretion in PM (Fig. 2G). One pivotal regulator for the inflammatory responses is the NF-κB signaling pathway. We performed a time course study of LPS treated PM to analyze the effect of MALAT1 ablation on NF-κB pathway. We found that MALAT1 ablation affected the classic NF-κB activation in that the phosphorylation of IKKα/β and phosphorylation of IκBα was reduced and IκBα protein level was increased in comparison with wild type (Fig. 2H). Furthermore, phosphorylation of p65 RelA was also reduced in MALAT1 ablated macrophages compared to wide type (Fig. 2H). Notably, among the pro-inflammatory cytokines regulated by MALAT1 ablation, IL-1β was the most profoundly inhibited cytokines compared to the other pro-inflammatory cytokines. Previous studies have shown that the maturation of IL-1β was predominately triggered by nucleotide-binding and oligomerization domain (NOD)-like receptor containing pyrin domain 3 (NLRP3) inflammasome, which is a multi-protein complex and could be activated by LPS, pathogen-associated molecular patterns (PAMP) and ROS. We tested if the NLRP3 inflammasome pathway was regulated in MALAT1 ablated macrophages by both qRT-PCR (Fig. 2I and J) and western blotting (Supplemental Fig. 2C). NLRP3 and caspase1 was significantly inhibited in MALAT1 ablated macrophage at both transcriptome and translation level, resulted in decreased IL-1β secretion.
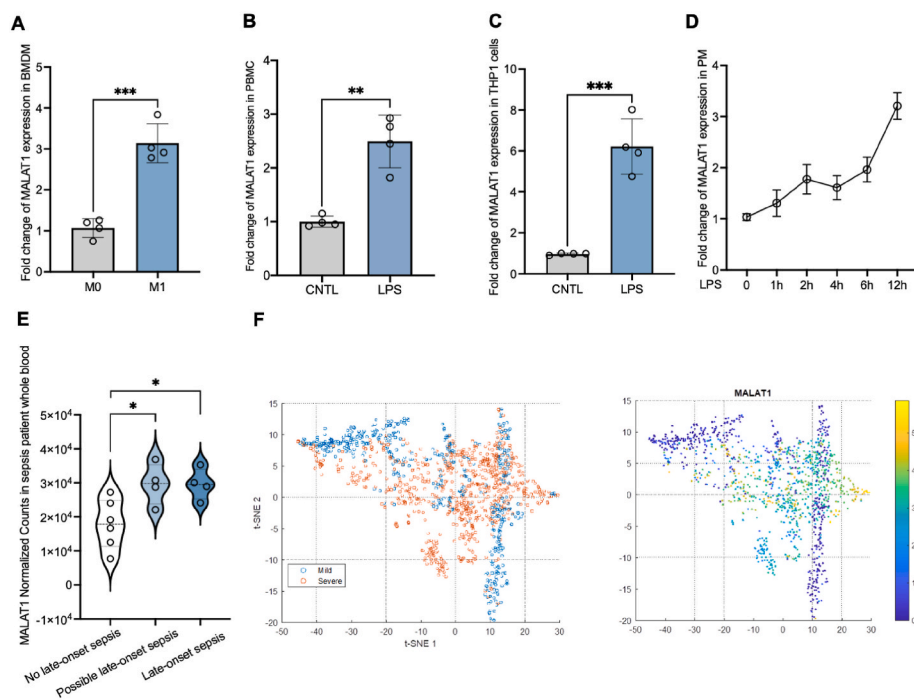

Fig. 1. MALAT1 is induced by sepsis process in both cells and sepsis patients.
A, MALAT1 expression level in mouse BMDM M0 (resting phase) and M1 (pro-inflammatory phase) determined by qRT-PCR. **B,** MALAT1 expression level in mouse PBMC treated with LPS (5 μg/mL, 12 h) determined by qRT-PCR. **C,** MALAT1 expression level in THP-1 derived macrophage treated with LPS (5 μg/mL, 12h) determined by qRT-PCR. **D,** Time-dependent MALAT1 expression level in mouse PM treated with LPS (5 μg/mL) determined by qRT-PCR. **E,** MALAT1 expression in transcriptomic analysis of whole blood sample from patient diagnosed with late-onset sepsis. **F,** MALAT1 expression visualized in t-distributed stochastic neighbor embedding (t-SNE) plot from in alveolar macrophages of COVID-19 with severe symptom than those with mild symptom.
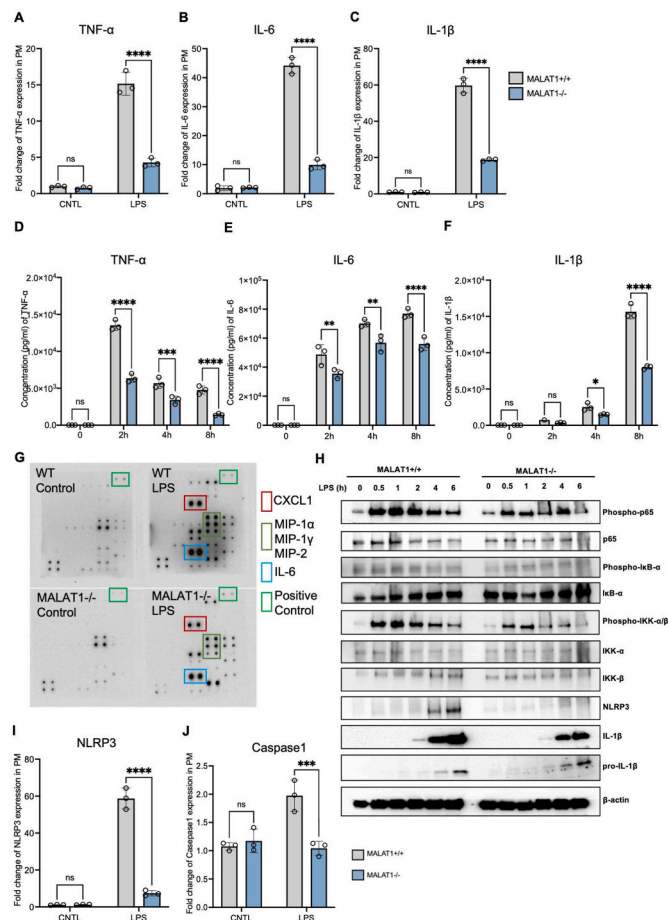
Fig. 2. Ablation of MALAT1 leads to inhibited proinflammatory response in peritoneal macrophages.
A-C, LPS induced pro-inflammatory gene expression in wild type (MALAT1+/+) and MALAT1 ablated (MALAT1−/−) PM treated with LPS (5 μg/mL) determined by qRT-PCR. D-F, Pro-inflammatory cytokine levels in the supernatant of PM isolated from MALAT1+/+ and MALAT1−/− mice treated with LPS (5 μg/mL, 0–8 h). G, Cytokine levels from culture supernatant of PM treated with LPS (5 μg/mL, 8 h) from both MALAT1+/+ and MALAT1−/− mice were determined using mouse cytokine array. H, NF-κB and NLRP3 inflammasome signaling pathway in PM treated with LPS (5 μg/mL, 0, 0.5, 1, 2, 4, 6 h) from MALAT1+/+ and MALAT1−/− mice. I and J, NLRP3 and Caspase1 gene expression level in MALAT1+/+ and MALAT1−/− PM treated with LPS (5 μg/mL, 6 h) determined by qRT-PCR.

3.3. MALAT1 null mice are highly resistant to LPS-induced endotoxemia and CLP-induced sepsis

It has been demonstrated that the severity of infections during sepsis is due to an activation cascade that will lead to an auto-amplifying cytokine production – the "cytokine storm" [43]. We profiled the 32 mouse cytokines in the plasma from the LPS-injected mice (i.p. injection, 30 mg/kg, 2 h) and found that MALAT1 ablation broadly inhibited proinflammatory cytokines and chemokines, including IL-6, CXCL1, and MIP-1 (Supplemental Fig. 2B). This observation is consistent with the culture supernatant from PM stimulated with LPS in vitro (Fig. 2G). With the observations that MALAT1 ablation reduced cytokine secretion in response to LPS in vitro and in vivo, we utilized two mouse sepsis model: 1) i.p. injection of LPS, and 2) CLP with 50% of ligation (Fig. 3B). Consistent with the cytokine profiling results, both sepsis models showed that MALAT1 null mice were highly resistant to the LPS-induced (Fig. 3A) and CLP-induced (Fig. 3C and D) sepsis with higher survival rate compared to wild type mice.

3.4. MALAT1 ablation enhanced antioxidant capacity through regulation of methionine/SAM pathway and attenuated proinflammatory response

Proinflammatory agents such LPS and cytokines have been found to cause severe oxidative stress with excessive generation of ROS during the progression of sepsis [44]. By performing a gene ontology analysis on a published data (GSE138712) of human whole blood from sepsis and healthy patients (on significant regulated genes, false discovery rate <0.05), we found cell redox homeostasis and cellular response to oxidative stress were ranking within top 10 significantly regulated pathways (Fig. 4A and Supplemental Fig. 3). This observation further supported the pivotal role oxidative stress played in sepsis. Interestingly, we found that MALAT1 ablation significantly attenuated ROS generation and reduced oxidative stress in PM (Fig. 4B) and BMDM (Supplemental Fig. 4), and increased the GSH/GSSG ratio and total GSH level in mice (Fig. 4D). The GSH/GSSG ratio has been considered as a useful estimation of the balance between oxidative reaction and endogenous antioxidant defense [45,46]. Cellular antioxidant defense including Nrf2 activation and GSH/GSSH pathway could counter inflammation by limiting ROS levels. The lower level of GSH has been found to augment inflammatory response in LPS/endotoxemia. Consistent with this observation, we found MALAT1 ablation increased GSH levels (Fig. 4D). One of the major determinants of GSH synthesis was transsulfuration pathway converting methionine to cysteine, which was then converted to GSH via GSH synthetic pathway. In the transsulfuration pathway, methionine is sequentially converted to cysteine via several enzymatic steps, among which the first and most important step is activation of methionine to SAM in a reaction catalyzed by MAT (Fig. 4C). Using cultured PM isolated from mice we found that methionine (1 mM, 6 h) and SAM (4 mM, 6 h) treatment reduced LPS-induced proinflammatory cytokine levels, meanwhile the MAT2A competitive inhibitor cLEU (30 mM, 6 h) increased proinflammatory cytokine levels, further supporting the role of methionine cycle in regulating inflammatory response in sepsis (Fig. 4E and F). In MALAT1 ablated PM, similar trend was detected by qRT-PCR (Supplemental Fig. 5).

3.5. MALAT1 regulates methionine pathway through m^6A modification in the highly conserved hairpin structure in MAT2A mRNA

Post-transcriptionally, the mRNA of MAT2A stability is regulated by the m^6A methylation mediated by RNA methylation writer METTL16 which methylates 3′UTR of MAT2A, thus controlling its level. Mechanistically, strong evidence from structural analysis indicates among the methylation sites of MAT2A, the hairpin1 is the linchpin for post-transcriptionally regulating MAT2A [47] by regulating intron splicing and mRNA decay [12,13], thus controlling methionine cycle (Fig. 5A and C). METTL16 also forms a complex with MALAT1 on the its 3′ region triple helix structure [15]. We found that in MALAT1 null mice, MAT2A expression was up regulated in both mRNA and protein level (Fig. 5B). Methylated RNA Immunoprecipitation (MeRIP) assay result suggested MALAT1 ablation counteracted the LPS-induced methylation near the MAT2A mRNA stop codon where the hairpin1 is located (Fig. 5D). By using a T3 ligation-dependent PCR assay (Fig. 6A), we analyzed the m^6A methylation level on MAT2A hairpin1 site. Interestingly, we found MALAT1 ablation in BMDM significantly increased the ligation efficiency, indicating decreased m^6A methylation level on the hairpin1 site of MAT2A in MALAT1 ablated BMDM (Fig. 6B). Using m^6A methylation RNA immunoprecipitation, we confirmed the increased m^6A methylation level in MAT2A hairpin1 site in wild type BMDM compared to MALAT1 null BMDM (Fig. 6C). Similar results were also observed in human THP-1 derived macrophage (Fig. 6D and E). Since m^6A methylation of MAT2A is associated with its decreased mRNA stability [12,13], this lower level of m^6A methylation in MALAT1 null mice is also consistent with higher protein level (Fig. 5B). We analyzed the role of MALAT1 in regulating MAT2A mRNA stability with actinomycin D treated BMDM. LPS treatment was found to accelerate mRNA decay,
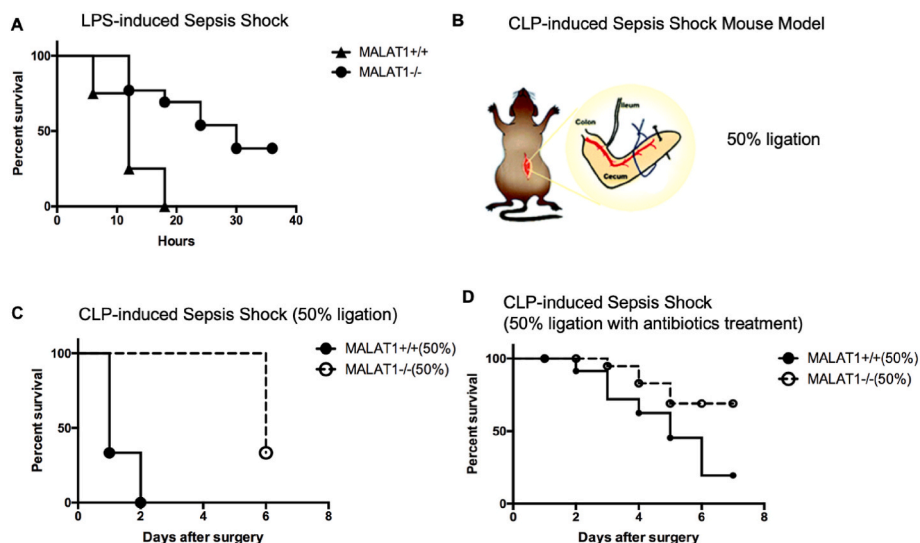
Fig. 3. MALAT1 ablation alleviates septic shock and increases the survival rate in both LPS-induced and CLP-induced mouse sepsis model.
A, Kaplan-Meier survival curves of MALAT1 ablated mice (n = 13) and wild type controls (n = 8) in response to i.p. injection of LPS, $p = 0.0016$ determined by Gehan-Breslow-Wilcoxon test. **B,** CLP induced mouse sepsis model. The ligation percentage of the cecum is 50%. **C,** Kaplan-Meier survival curves of MALAT1 ablated mice (n = 6) and wild type mice (n = 6) in 50% CLP-induced sepsis model, $p = 0.0013$ determined by Gehan-Breslow-Wilcoxon test. **D,** Kaplan-Meier survival curves of MALAT1 ablated mice (n = 16) and wild type mice (n = 11) in the CLP-induced sepsis model with antibiotics treatment, $p = 0.0281$ determined by Gehan-Breslow-Wilcoxon test.
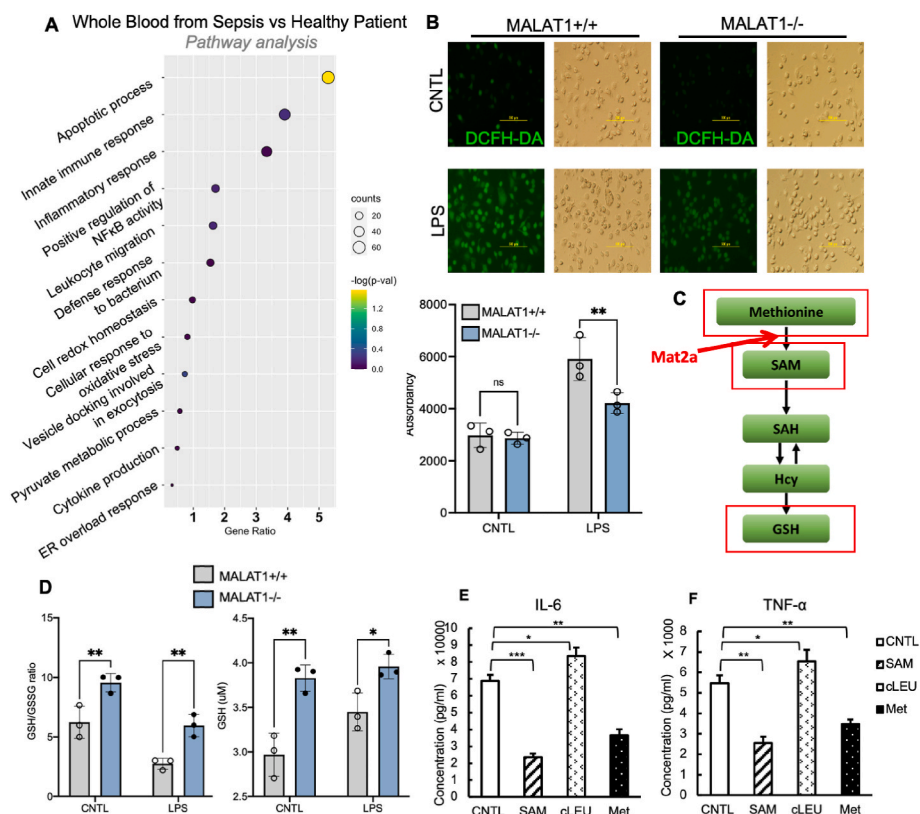

Fig. 4. MALAT1 ablation enhanced antioxidant capacity through regulation of methionine/SAM pathway and attenuated proinflammatory response.
A, Enriched pathway analysis in aortic intima from sepsis patients versus healthy controls. **B,** ROS levels in MALAT1 null and wild type PM challenged with LPS (5 μg/mL, 12 h) were determined by both immunofluorescence microscopy and fluorescence quantification with plate reader (BioTek) using H2-DCFH-DA as a fluorescent dye. **C,** Schematic illustration of methionine/SAM/GSH pathway. **D,** GSH/GSSG ratio and total GSH level in MALAT1 null and wild type PM. **E-F,** IL-6 and TNF-α level in the supernatant of PM co-treated with LPS (5 μg/mL) and methionine (1 mM), SAM (4 mM), cLEU (30 mM) for 6 h.

while MALAT1 ablation was found to increase MAT2A mRNA half-life, indicating higher mRNA stability (Supplemental Fig. 5C).

Importantly, we found that enhancement of methionine pathway by supplement of methionine (gavage, 20 mg/kg) significantly increased the survival rate in CLP-induced mouse sepsis model (Fig. 7A), and supplement of cysteine (gavage, 20 mg/kg) also increased the survival rate of LPS-induced endotoxemia (Supplemental Fig. 6B). On the contrary, treatment of cLEU (i.p. injection, 400 mg/kg) decreased survival rate in CLP-induced mouse sepsis model (Supplemental Fig. 6A). These results suggest that MALAT1 regulates methionine/SAM biosynthesis by post-transcriptionally regulating MAT2A, and that MALAT1-regulated methionine metabolism pathway can be of great value in the

treatment of sepsis (Fig. 7B).

4. Discussion

In addition to its well-recognized role in cancer progression, MALAT1 has recently been found to play an important role in increasingly wide range of diseases and their progressions including diabetes and its associated complications [30,48], inflammatory diseases as in COVID-19 [49,50] and sepsis [27,50]. One commonality underpinning many of the physiological functions of MALAT1 is its ability to regulate the oxidative stress responses which is pivotal point of convergent of many pathophysiological processes. Genomic study empowered by the
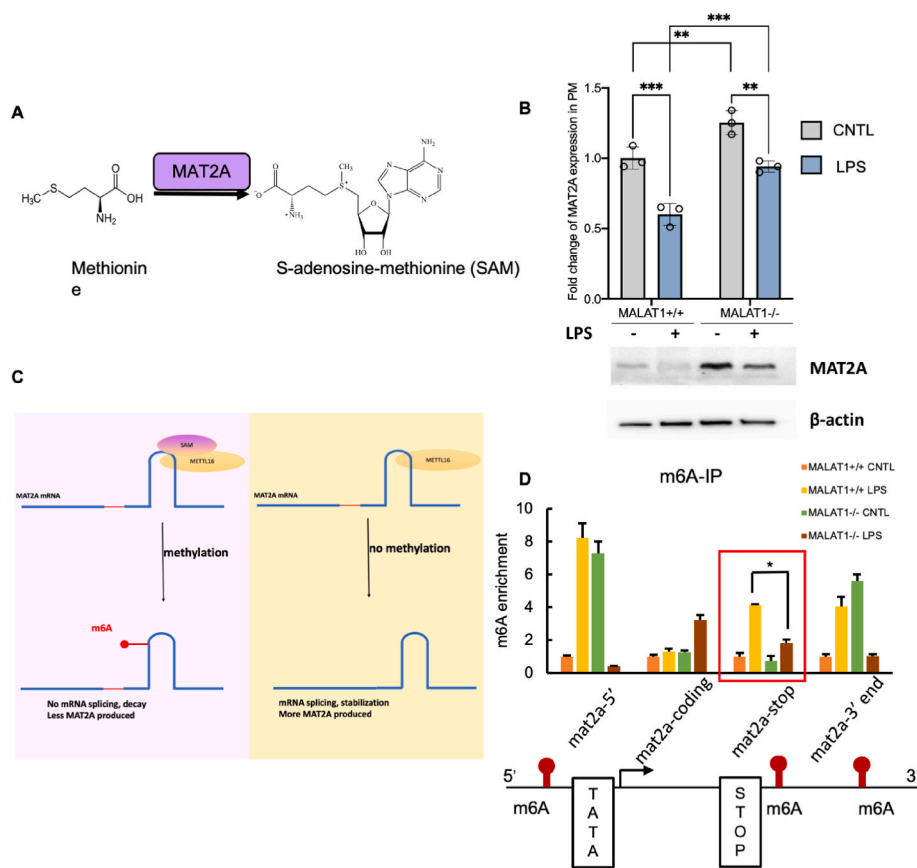
Fig. 5. MALAT1 regulate MAT2A expression level through m⁶A methylation on MAT2A mRNA.
A, MAT2A as a key enzyme to catalyze methionine to SAM. **B,** MAT2A gene and protein expression in PM treated with LPS (5 μg/mL) in MALAT1+/+ and MALAT1−/− mice. *p* value was determined two-way ANOVA with Fisher's test. **C,** METTL16 catalyzes methylation of MAT2A, leading to mRNA decay. **D,** m⁶A methylation enrichment on MAT2A mRNA under treatment of LPS in wild type and MALAT1 ablated PM.
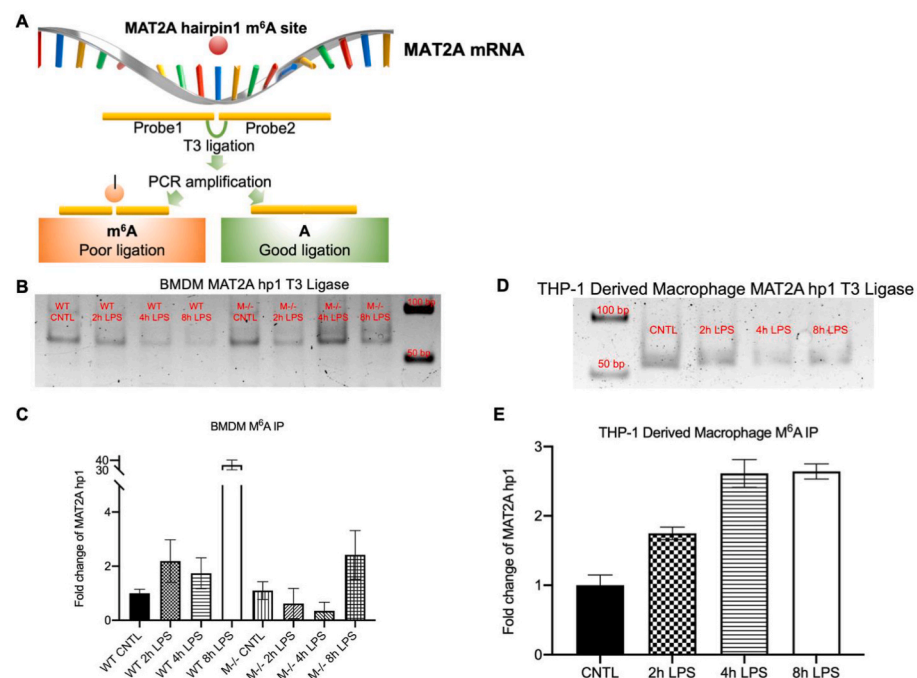

Fig. 6. MALAT1 epitranscriptomically regulates MAT2A expression level through m⁶A methylation on MAT2A mRNA.
A, Schematic illustration of T3 ligation-dependent PCR assay for m⁶A detection on the MAT2A gene. **B,** Gel electrophoresis for identifying m⁶A event using T3 ligation-dependent PCR of MAT2A hairpin1 in BMDM from wild type and MALAT1 null mice. **C,** m⁶A methylation enrichment on MAT2A hairpin1 under treatment of LPS in wild type and MALAT1 ablated BMDM under a time-dependent manner. **D,** Gel electrophoresis for identifying m⁶A event using T3 ligation-dependent PCR of MAT2A hairpin1 in THP-1 derived macrophages treated with LPS (5 μg/mL). **E,** m6A methylation enrichment on MAT2A hairpin1 under treatment of LPS in THP-1 derived macrophages under a time-dependent manne.

next generation sequencing technology reveals that MALAT1 is pervasively associated with genomes in the regions critical for transcriptional regulation as well as RNA processing, suggesting a pleiotropic role of MALAT1 in regulating gene expression and signaling pathways under various pathophysiological conditions [51]. The pleiotropy of MALAT1 may also stem from its ability in regulating gene expression at post-transcriptional as well as transcriptional levels. Recent studies suggest that MALAT1 regulates gene expression at post-transcriptional level through its interaction with m⁶A RNA methyltransferase METTL16, thus adding a new dimension as a regulator for
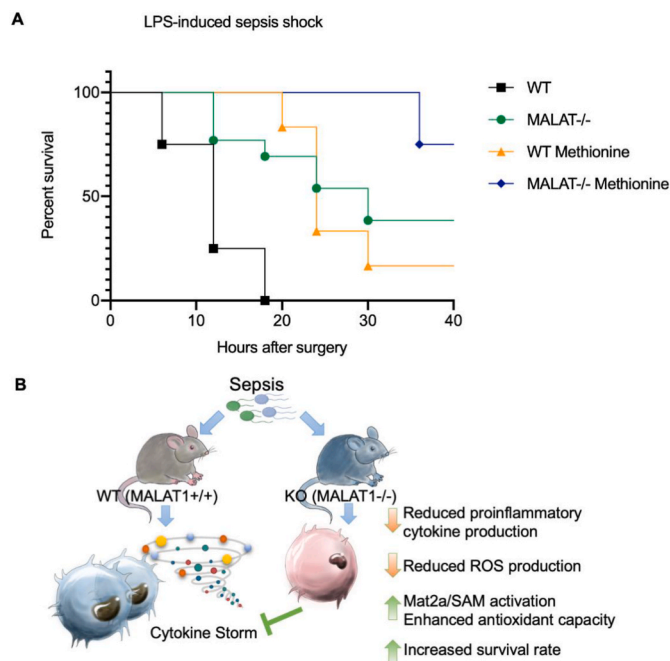
Fig. 7. MALAT1 ablation alleviates cytokine storm and increase the survival rate during sepsis through regulating methionine/SAM pathway. A, Kaplan-Meier survival curves of wild type and MALAT1 null mice administered with methionine (20 mg/kg) via gavage in the CLP-induced sepsis model (WT n = 8, MALAT1−/− n =13, WT methionine n = 6, MALAT1−/− methionine n = 8. $p < 0.0001$, determined by Gehan-Breslow-Wilcoxon test). **B,** Illustration of MALAT1 ablation alleviates cytokine storm and increased survival rate in mouse sepsis model.

epitranscriptomic regulation of gene expressions [15].

In this study, we used the constitutive MALAT1 null mouse model to investigate the role of MALAT1 in regulation of inflammatory responses in the progression of sepsis. In mouse BMDM, as well as human THP-1 derived macrophage, MALAT1 is highly expressed in the M1 proinflammatory phase as compared to the M0 resting phase (Fig. 1A–C) and MALAT1 expression is also swiftly increased in response to the LPS treatment in mouse PM (Fig. 1D). In transcriptomic analysis of human clinical samples, MALAT1 expression is highly induced in human peripheral blood with late-onset sepsis (Fig. 1E), alveolar macrophages of sever symptom COVID-19 (Fig. 1F), and also in human bone marrow treated with LPS (Supplemental Fig. 1). These results are consistent with the role of MALAT1 in regulating inflammatory responses and also providing evidence for its prognostic value for sepsis (Fig. 1E) [35]. In analyzing the inflammatory responses, we have detected a broad increase in proinflammatory cytokines as determined in serum samples of endotoxemia mice as well as in PM. Notably, striking reductions in proinflammatory cytokine levels were observed in MALAT1 null mice compared to wild type mice indicating a much-subdued cytokine storm in the absence of MALAT1 (Fig. 2 and Supplemental Fig. 2).

Our results suggest MALAT1 regulates signaling pathways involved in inflammatory response, including both the NF-κB and NLRP3 inflammasome pathways. In response to LPS induced endotoxemia, the innate immune system such as macrophages is activated through NF-κB pathway which activates NLRP3 inflammasome through two step signal processes where LPS activates NF-κB pathway followed by the activation of caspase1 leading to the processing of pro-IL-1β and assembly of NLRP3 inflammasome [52]. Indeed, our observations with the macrophage were consistent with this process where the classic NF-κB pathway was activated with high level of NLRP3 and IL-1β expression indicating the activation of the NLRP3 inflammasome. The LPS-induced NF-κB activation and subsequent caspase1 and NLRP3 levels were greatly reduced in MALAT1 ablated macrophage (Fig. 2H–J,

Supplemental Fig. 2C).

Oxidative stress induced by the inflammatory responses goes hand-in-hand in sepsis [6]. In fact, it forms a positive feedback loop during the inflammatory responses [52]. In pathway analysis, we analyzed clinical sepsis patient samples and showed that the expression of MALAT1 was upregulated, which coincided with the activation of the oxidative stress and inflammatory pathways (Fig. 4A and Supplemental Fig. 3). The endotoxemia-induced oxidative stress/ROS could be clearly observed in the mouse PM and MALAT1 ablation greatly reduced oxidative stress/ROS levels in the MALAT1−/− macrophages (Fig. 4B and Supplemental Fig. 4), which was consistent with the reduction of proinflammatory cytokines (Fig. 2 and Supplemental Fig. 2) and reduced lethality in mouse sepsis model (Figs. 3 and 7A). In fact, MALAT1 ablated macrophages showed higher antioxidant capacity with much reduced background level of oxidative stress without septic challenges (Fig. 4B and Supplemental Fig. 4). This salient feature of MALAT1 ablation may be due to enhanced antioxidant pathways regulated by the master regulator Nrf2 as we have shown in our earlier study [30] and increased methionine cycle regulated by MAT2A as shown in this study.

Oxidative stress and its associated excessive ROS is normally neutralized by antioxidants, among which GSH is the most abundant [53,54]. Consistent with much reduced oxidative stress/ROS in MALAT1 null macrophages, we have observed a greatly increased GSH/GSSG ratio and total GSH level, indicating increased antioxidant capacity in MALAT1 null macrophages (Fig. 4D). Glutathione is the product from methionine cycle. One critical step for the methionine cycle is the synthesis of SAM from methionine and ATP, catalyzed by MAT2A (Fig. 4C). SAM is an important precursor of GSH which has been shown to ameliorate LPS-induced hepatotoxicity [45]. Consistent with this observation, we found that in vitro treatment of methionine and SAM could reduce LPS-induced proinflammatory cytokine production in mice PM (Fig. 4E and F and Supplemental Fig. 5), and that supplement of methionine by gavage significantly increased the survival rate of both wild type and MALAT1 ablated mice during CLP-induced sepsis (Fig. 7A). Furthermore, treatment of cLEU, which is an enzymatic inhibitor of MAT2A, significantly increased LPS-induced proinflammatory cytokine production in mice PM (Fig. 4E and F and Supplemental Fig. 5), and i.p. injection of cLEU significantly decreased mice survival rate during LPS-induced endotoxemia (Supplemental Fig. 6A). These findings indicate that methionine cycle plays a significant role in regulating inflammatory responses in sepsis by modulating antioxidant capacity.

As a key enzyme in methionine cycle, MAT2A is regulated by MALAT1, as MALAT1 ablation significantly increased MAT2A gene expression and translation (Fig. 5B). Mechanistically, MAT2A is post-transcriptionally regulated by METTL16 through m6A methylation of its 3′UTR, which will lead to intron retention and nuclear degradation of MAT2A transcript [12] (Fig. 5C). We hypothesize that by binding to METTL16, MALAT1 can impact on the m6A methylation on hairpin1 site of MAT2A, and in turn regulates MAT2A protein level. We found that MAT2A expression was significantly suppressed under endotoxemia condition, while MALAT1 ablation alleviated this LPS-induced suppression (Fig. 5B). To test the m6A methylation events on MAT2A mRNA, we first performed MeRIP, and found that LPS-treatment caused increases in m6A methylation, especially near the stop codon of the MAT2A mRNA where the hairpin1 is located, and that m6A methylation was greatly reduced in MALAT1 ablated PM and BMDM (Fig. 5D). To pinpoint the site of methylation, we further analyzed the m6A methylation at single nucleotide resolution by the T3 ligation-dependent PCR assay (Fig. 6A). Confirmed by both m6A IP assay and T3 ligation-dependent PCR assay, we observed that MAT2A hairpin1 m6A methylation increased by LPS treatment, and MALAT1 ablation significantly reduced this increase (Fig. 6). It has been shown that excessive m6A modification is detrimental for the translation [55], therefore it is possible that the higher MAT2A mRNA methylation level observed in wide type macrophages inhibited its translation in addition to reducing

mRNA level, thus causing a larger reduction in protein level (Fig. 5B). These findings suggest a working model where MALAT1 post-transcriptionally regulates MAT2A through binding of METTL16, leading to m6A methylation which in turn regulates MAT2A protein level. By regulating this key enzyme in methionine/SAM biosynthesis process, MALAT1 regulates inflammatory response as MALAT1 ablation significantly increased the survival rates of mice during both CLP-induced sepsis and LPS-induced endotoxemia (Figs. 3 and 7A).

In conclusion, these exciting results suggested that MALAT1 regulates NF-κB and NLRP3 inflammasome signaling pathway, and methionine metabolism pathway in the progression of acute inflammatory responses during sepsis. Our findings provide novel insights in searching of therapeutic targets to alleviate sepsis, such as antisense therapeutics against MALAT1 and/or through enhancing the methionine cycle.

Author contributions

Conceived and designed the experiments: JC ST YT. Performed the experiments: JC ST SK. Analyzed the data: JC ST JJC DO YT. Contributed reagents/materials/analysis tools: AG BM GAC MW SG YS. Wrote the paper: JC ST YT. Provided study supervision: YT.

Declaration of competing interest

The authors have declared that no conflict of interest exists.

Acknowledgments

Appendix A. Supplementary data

Supplementary data to this article can be found online at https://doi.org/10.1016/j.redox.2022.102377.

References

[1] Q. Yang, et al., The role of tyrosine phosphorylation of protein kinase C delta in infection and inflammation, Int. J. Mol. Sci. 20 (6) (2019) 1498.

[2] J.A. Hippensteel, et al., Circulating heparan sulfate fragments mediate septic cognitive dysfunction, J. Clin. Invest. 129 (4) (2019) 1779–1784.

[3] H.B. Nguyen, et al., Severe sepsis and septic shock: review of the literature and emergency department management guidelines, Ann. Emerg. Med. 48 (1) (2006) 54, e1.

[4] H.C. Prescott, D.C. Angus, Enhancing recovery from sepsis: a review, JAMA 319 (1) (2018) 62–75.

[5] H.F. Galley, Oxidative stress and mitochondrial dysfunction in sepsis, Br. J. Anaesth. 107 (1) (2011) 57–64.

[6] H. Nagar, S. Piao, C.-S. Kim, Role of mitochondrial oxidative stress in sepsis, Acute Crit Care. 33 (2) (2018) 65.

[7] L. Lauinger, P. Kaiser, Sensing and signaling of methionine metabolism, Metabolites 11 (2) (2021) 83.

[8] S.C. Lu, J.M. Mato, Role of methionine adenosyltransferase and S-adenosylmethionine in alcohol-associated liver cancer, Alcohol 35 (3) (2005) 227–234.

[9] S.A. Lozano-Sepulveda, et al., S-adenosyl-L-methionine modifies antioxidant-enzymes, glutathione-biosynthesis and methionine adenosyltransferases-1/2 in hepatitis C virus-expressing cells, World J. Gastroenterol. 22 (14) (2016) 3746.

[10] S.C. Lu, H. Tsukamoto, J.M. Mato, Role of abnormal methionine metabolism in alcoholic liver injury, Alcohol 27 (3) (2002) 155–162.

[11] K.S.K. Seo Yeon Lee, Protective effects of S-adenosylmethionine and its combinations with taurine and/or betaine against lipopolysaccharide or polyinosinic-polycytidylic acid-induced acute hepatotoxicity, J Cancer Prev. 21 (3) (2016).

[12] K.E. Pendleton, et al., The U6 snRNA m6A methyltransferase METTL16 regulates SAM synthetase intron retention, Cell 169 (5) (2017) 824–835, e14.

[13] H. Shima, et al., S-Adenosylmethionine synthesis is regulated by selective N6-adenosine methylation and mRNA degradation involving METTL16 and YTHDC1, Cell Rep. 21 (12) (2017) 3354–3363.

[14] A.S. Warda, et al., Human METTL16 is a N6-methyladenosine (m6A) methyltransferase that targets pre-mRNAs and various non-coding RNAs, EMBO Rep. 18 (11) (2017) 2004–2014.

[15] J.A. Brown, et al., Methyltransferase-like protein 16 binds the 3′-terminal triple helix of MALAT1 long noncoding RNA, Proc. Natl. Acad. Sci. USA 113 (49) (2016) 14013–14018.

[16] L. Statello, et al., Gene regulation by long non-coding RNAs and its biological functions, Nat. Rev. Mol. Cell Biol. 22 (2) (2021) 96–118.

[17] T. Hung, H.Y. Chang, Long noncoding RNA in genome regulation: prospects and mechanisms, RNA Biol. 7 (5) (2010) 582–585.

[18] S. Biswas, et al., MALAT1: an epigenetic regulator of inflammation in diabetic retinopathy, Sci. Rep. 8 (1) (2018) 1–15.

[19] G. Arun, D. Aggarwal, D.L. Spector, MALAT1 long non-coding RNA: functional implications, Non-coding RNA 6 (2) (2020) 22.

[20] Y.G. Chen, A.T. Satpathy, H.Y. Chang, Gene regulation in the immune system by long noncoding RNAs, Nat. Immunol. 18 (9) (2017) 962–972.

[21] J. Chen, L. Ao, J. Yang, Long non-coding RNAs in diseases related to inflammation and immunity, Ann. Transl. Med. 7 (18) (2019).

[22] J.L. Rinn, H.Y. Chang, Long noncoding RNAs: molecular modalities to organismal functions, Annu. Rev. Biochem. 89 (2020) 283–308.

[23] H. Chen, et al., LncRNA THRIL aggravates sepsis-induced acute lung injury by regulating miR-424/ROCK2 axis, Mol. Immunol. 126 (2020) 111–119.

[24] Q. Huang, et al., Circulating lncRNA NEAT1 correlates with increased risk, elevated severity and unfavorable prognosis in sepsis patients, Am. J. Emerg. Med. 36 (9) (2018) 1659–1663.

[25] H. Wu, et al., LncRNA-HOTAIR promotes TNF-α production in cardiomyocytes of LPS-induced sepsis mice by activating NF-κB pathway, Biochem. Biophys. Res. Commun. 471 (1) (2016) 240–246.

[26] G. Zhao, et al., The long noncoding RNA MALAT 1 regulates the lipopolysaccharide-induced inflammatory response through its interaction with NF-κB, FEBS Lett. 590 (17) (2016) 2884–2895.

[27] F. Geng, W. Liu, L. Yu, Potential role of circulating long noncoding RNA MALAT1 in predicting disease risk, severity, and patients' survival in sepsis, J. Clin. Lab. Anal. 33 (8) (2019), e22968.

[28] S.B. Huachun Cui, Sijia Guo, Na Xie, Jing Ge, Dingyuan Jiang, Zörnig Martin, Victor J. Thannickal, Gang Liu, Long noncoding RNA Malat1 regulates differential activation of macrophages and response to lung injury, JCI insight 4 (4) (2019).

[29] Y.-X.Z. Bo Shu, Hao Li, Rui-Zhi Zhang, Chao He, Xin Yang, The METTL3/MALAT1/PTBP1/USP8/TAK1 axis promotes pyroptosis and M1 polarization of macrophages and contributes to liver fibrosis, Cell Death Discov. 7 (368) (2021).

[30] J. Chen, et al., Long noncoding RNA MALAT1 regulates generation of reactive oxygen species and the insulin responses in male mice, Biochem. Pharmacol. 152 (2018) 94–103.

[31] S. Ng, et al., Whole blood transcriptional responses of very preterm infants during late-onset sepsis, PLoS One 15 (6) (2020), e0233841.

[32] X. Huang, M. Zhao, High expression of long non-coding RNA MALAT1 correlates with raised acute respiratory distress syndrome risk, disease severity, and increased mortality in septic patients, Int. J. Clin. Exp. Pathol. 12 (5) (2019) 1877.

[33] W. Liu, F. Geng, L. Yu, Long non-coding RNA MALAT1/microRNA 125a axis presents excellent value in discriminating sepsis patients and exhibits positive association with general disease severity, organ injury, inflammation level, and mortality in sepsis patients, J. Clin. Lab. Anal. (2020), e23222.

[34] M.M. Parker, et al., RNA sequencing identifies novel non-coding RNA and exon-specific effects associated with cigarette smoking, BMC Med. Genom. 10 (1) (2017) 58.

[35] J. Chen, et al., Long non-coding RNA MALAT serves as an independent predictive biomarker for the diagnosis, severity and prognosis of patients with sepsis, Mol. Med. Rep. 21 (3) (2020) 1365–1373.

[36] J.Y. Weiliang Liu, Zhenhao Zhang, Hongru Pian, Chenghui Liu, Zhengping Li, Identification of a selective DNA ligase for accurate recognition and ultrasensitive quantification of N 6 -methyladenosine in RNA at one-nucleotide resolution, Chem. Sci. 9 (2018) 3354–3359.

[37] M.S. Antonio Layoun, Manuela M. Santos, Isolation of murine peritoneal macrophages to carry out gene expression analysis upon toll-like receptors stimulation, JoVE 98 (2015), e52749.

[38] P.S.C. Wei Ying, W. Bazer Fuller, H. Safe Stephen, Zhou Beiyan, Investigation of macrophage polarization using bone marrow derived macrophages, J Visualized Experiments 76 (2013), e50323.

[39] L.M. Swift, N. Sarvazyan, Localization of dichlorofluorescin in cardiac myocytes: implications for assessment of oxidative stress, Am. J. Physiol. Heart Circ. Physiol. 278 (3) (2000) H982–H990.

[40] Y. Tian, et al., Ah receptor and NF-κB interactions, a potential mechanism for dioxin toxicity, J. Biol. Chem. 274 (1) (1999) 510–515.

[41] M. Reyes, M.R. Filbin, R.P. Bhattacharyya, K. Billman, T. Eisenhaure, D.T. Hung, B. D. Levy, R.M. Baron, P.C. Blainey, M.B. Goldberg, N. Hacohen, An immune-cell signature of bacterial sepsis, Nat. Med. 26 (2020) 333–340.

[42] L. Cheng, et al., Whole blood transcriptomic investigation identifies long non-coding RNAs as regulators in sepsis, J. Transl. Med. 18 (2020) 1–13.

[43] B.G. Chousterman, F.K. Swirski, G.F. Weber, Cytokine storm and sepsis disease pathogenesis, in: Seminars in Immunopathology, Springer, 2017.

[44] J. Tschopp, K. Schroder, NLRP3 inflammasome activation: the convergence of multiple signalling pathways on ROS production? Nat. Rev. Immunol. 10 (3) (2010) 210–215.

[45] K. Ko, et al., Changes in S-adenosylmethionine and GSH homeostasis during endotoxemia in mice, Lab. Invest. 88 (10) (2008) 1121–1129.

[46] H.J. Forman, H. Zhang, A. Rinna, Glutathione: overview of its protective roles, measurement, and biosynthesis, Mol. Aspect. Med. 30 (1–2) (2009) 1–12.

[47] K.A. Doxtader, et al., Structural basis for regulation of METTL16, an S-adenosylmethionine homeostasis factor, Mol. Cell 71 (6) (2018) 1001–1011, e4.

[48] W. Ye, et al., LncRNA MALAT1 regulates miR-144-3p to facilitate epithelial-mesenchymal transition of lens epithelial cells via the ROS/NRF2/Notch1/Snail pathway, Oxid. Med. Cell. Longev. (2020) 2020.

[49] A.C. Rodrigues, et al., NEAT1 and MALAT1 are highly expressed in saliva and nasopharyngeal swab samples of COVID-19 patients, Mol oral Microbiol. 36 (6) (2021) 291–294.

[50] K. Huang, et al., Long non-coding RNAs (lncRNAs) NEAT1 and MALAT1 are differentially expressed in severe COVID-19 patients: an integrated single-cell analysis, PLoS One 17 (1) (2022) e0261242.

[51] J.M. Engreitz, et al., RNA-RNA interactions enable specific targeting of noncoding RNAs to nascent Pre-mRNAs and chromatin sites, Cell 159 (1) (2014) 188–199.

[52] A. Dominic, N.-T. Le, M. Takahashi, Loop between NLRP3 inflammasome and reactive oxygen species, Antioxidants Redox Signal. (2021) ja.

[53] N. Ballatori, et al., Glutathione dysregulation and the etiology and progression of human diseases, 2009.

[54] P. Kumar, et al., Severe glutathione deficiency, oxidative stress and oxidant damage in adults hospitalized with COVID-19: implications for GlyNAC (Glycine and N-acetylcysteine) supplementation, Antioxidants 11 (1) (2022) 50.

[55] R.H. Boris Slobodin, Calderone Vittorio, A.F. Joachim, Oude Vrielink, Fabricio Loayza-Puch, Elkon Ran, Reuven Agami, Transcription impacts the efficiency of mRNA translation via Co-transcriptional N6-adenosine methylation, Cell 169 (2) (2017).